Available online at www.sciencedirect.com
SCIENCE DIRECT
Tetrahedron: Asymmetry
Tetrahedron: *Asymmetry* 17 (2006) 1846–1852

Enantiomer separation by enantioselective inclusion complexation–organic solvent nanofiltration

Nazlee F. Ghazali,[a] Frederico C. Ferreira,[a] Andrew J. P. White[b] and Andrew G. Livingston[a,*]

[a]*Department of Chemical Engineering, Imperial College, London SW7 2AZ, UK*
[b]*Department of Chemistry, Imperial College, London SW7 2AZ, UK*

Received 18 May 2006; accepted 16 June 2006

Abstract—A novel chiral separation process, which utilizes a combination of enantioselective inclusion complexation (EIC) and organic solvent nanofiltration (OSN), was developed. Although EIC is an attractive way to resolve racemates, the difficulties associated with enantiomer recovery and chiral host recycle has limited large-scale applications. EIC coupled with OSN replaces distillation for the recovery of enantiomers from enantioenriched solid complex. A decomplexation solvent is employed to dissociate enantiomers from the complex, and subsequent separation of enantiomers from the chiral host is realized using OSN. The new process was investigated using racemic 1-phenylethanol as the guest and (*R*,*R*)-TADDOL as the chiral host. This novel technology expands the application of EIC to the resolution of nonvolatile racemates, and enables large-scale application.

1. Introduction

Resolution via diastereomeric salt formation remains common in large-scale production of optically pure enantiomers due to its operational simplicity and reliability.[1] However, it is limited to the resolution of acids and bases. Enantioselective inclusion complexation (EIC) is a promising technique which, since it is not restricted to proton transfer interactions, can in principle be used to resolve compounds with almost any functional group.[2] Numerous successful resolutions have been reported by Toda and co-workers[3] together with other novel developments,[4] although we also note that some recent investigations[5] report a less optimistic view of the scope of EIC. Nevertheless, versatile chiral hosts such as TADDOLs are excellent in terms of resolving structurally similar alcohols, ketones, amines, sulfoxides and amino acid esters.[6] However, an outstanding difficulty with EIC is the separation of enantiomers from the enantioenriched solid complex, which is typically performed by distillation. This limits EIC to the separation of enantiomers with appreciable volatility. Even for these it would be difficult to operate at large scale due to high temperature distillation, with its concomitant problematic heat transfer and vacuum conditions. Here we report, for the first time, a novel enantioseparation process, which combines the highly enantioselective nature of inclusion complexation with the subsequent separation of enantiomers from a chiral host using solvent decomplexation and organic solvent nanofiltration (OSN). In our proposed process (Fig. 1), a racemate is added to a chiral host suspended in a resolution solvent. The (*S*)-enantiomer enantioselectively co-crystallizes with the chiral host while the (*R*)-enantiomer remains in the liquid (Step A). Nanofiltration of the resulting resolution suspension elutes the (*R*)-enantiomer (Step B), retaining the chiral host and the chiral host–(*S*)-enantiomer complex. A decomplexation solvent is then added to dissolve and dissociate the complex into (*S*)-enantiomer and host (Step C). This solution is subsequently nanofiltered to elute the (*S*)-enantiomer, while the soluble host is retained by the membrane (Step D). Exchanging the decomplexation solvent for the resolution solvent via diafiltration with the resolution solvent causes the host to recrystallize (Step E), and it is returned to the next cycle. The ambient operating temperature and simplicity of OSN separations make combined EIC–OSN ideal for the separation of nonvolatile and labile enantiomers. Since chiral hosts are used in stoichiometric quantities, their recovery and multiple reuse is a further key advantage of separation by OSN.

To demonstrate this process, we used *rac*-phenylethanol **1** (122 g mol^{-1}) as a racemate and (4*R*,5*R*)-(−)-2,2-di-

* Corresponding author. Tel.: +44 20 7594 5582; fax: +44 20 7594 5629; e-mail: a.livingston@ic.ac.uk

0957-4166/$ - see front matter © 2006 Elsevier Ltd. All rights reserved.
doi:10.1016/j.tetasy.2006.06.026

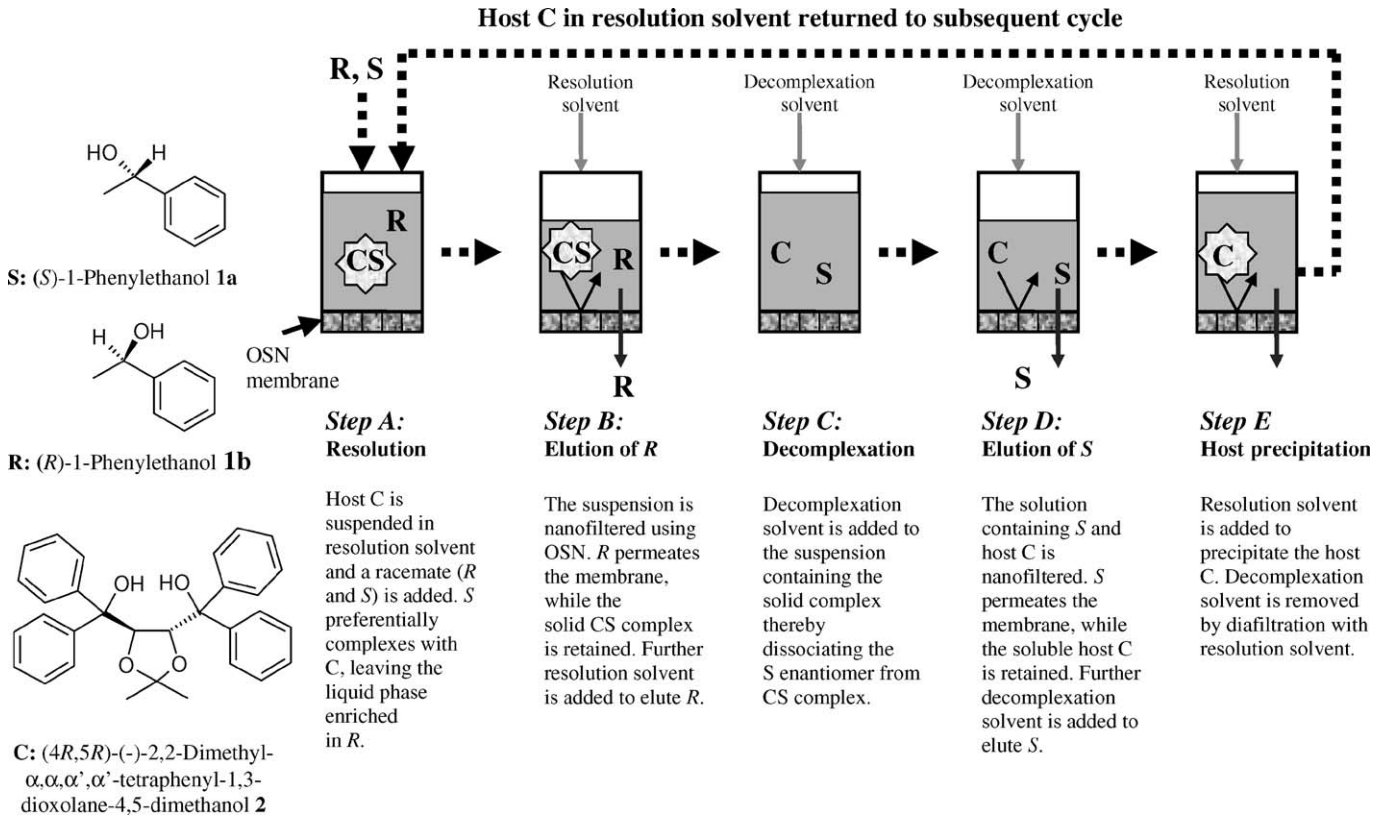

Figure 1. Process schematic of enantioselective inclusion complexation–organic solvent nanofiltration and structure of model host and enantiomers.

methyl-α,α,α′,α′-tetraphenyl-1,3-dioxolane-4,5-dimethanol [(*R*,*R*)-TADDOL] **2** (466 g mol^{-1}) as a chiral host.[7] A commercially available polyimide OSN membrane, STARMEM™ 122,[8] with a nominal molecular weight cutoff (MWCO) of 220 g mol^{-1} was used for OSN. These OSN membranes have been found to be effective for molecular level separations.[9] It was anticipated, based on MWCO,[10] that the host would be retained while the enantiomers would permeate freely. Hexane was used as the resolution solvent and toluene as the decomplexation solvent.

2. Results and discussion

Before performing the process, several fundamental phenomena such as the membrane separation characteristics of racemate and chiral host, solid-state properties of the solid complex, kinetics of resolution, effect of solvent composition on decomplexation and parameters affecting resolution were investigated. Racemic **1** was highly permeable in the OSN membrane, and had zero rejection[11] in both toluene and hexane. Chiral host **2** was retained efficiently by the OSN membrane (>99% rejection in both solvents). The resolution of **1** with **2** was rapid and reached equilibrium after 1 h, based on measurements of the enantiomeric excess of the mother liquor. Crystals of **2** initially present as a suspension in hexane were easily observed under a microscope, but upon the addition of **1** the solid was converted into a far more finely divided material for which crystals could not be seen. However, powder X-ray diffraction patterns showed that the solids formed after addition of **1** possessed a degree of crystallinity, suggesting that a change of crystal structure had occurred upon the addition of **1** to crystalline **2**.

For the X-ray crystal structure determination, single crystals were obtained by recrystallizing the crude inclusion complex from a 1:2 (v/v) toluene/hexane mixture. The X-ray crystal structure of the 2:1 inclusion complex formed between host **2** and guest **1a** is shown in Figure 2. The dominant feature is the formation of a five O–H···O hydrogen bond ring formed from two intramolecular linkages between the hydroxyl groups of each host **2** molecule (interactions a and b), one intermolecular host **2**···host **2** linkage (interaction c) and two linkages between the included guest **1a** and host **2** molecules (interactions d and e). It has previously been shown that in the absence of a guest molecule, host **2** crystallizes in a somewhat similar fashion, with two independent molecules forming a four O–H···O hydrogen bond 'square' (see Fig. 3).[12] The addition of guest **1a** effectively results in one side of this square 'opening up' to accommodate the extra OH moiety (breaking one O–H···O linkage and forming two new ones), with one of the host **2** molecules (the one on the right hand side of both Figs. 2 and 3) taking up a noticeably different orientation. Interestingly, the inclusion complex formed between (*S*)-phenylethylamine (essentially just changing the OH in guest **1a** for an NH_2) and host **2** is almost identical.[13]

From an inspection of Figure 2 it is evident that the involvement of the hydroxyl moiety of the guest in the

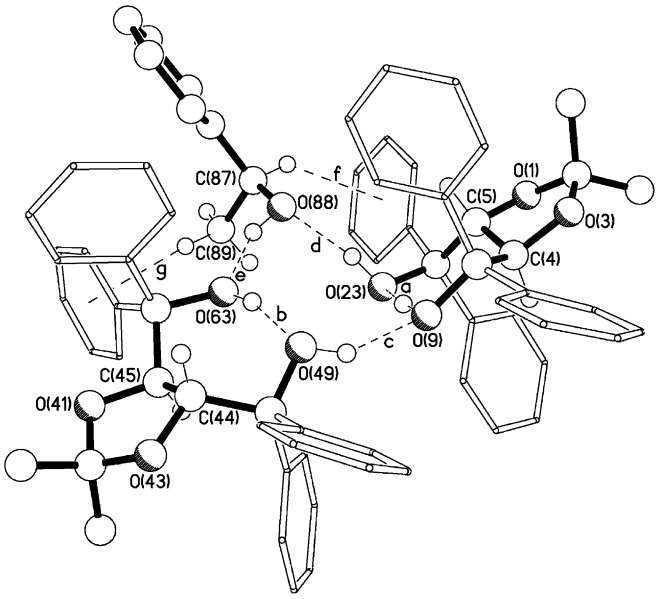

Figure 2. The molecular structure of inclusion complex $[\mathbf{2}]_2{\cdot}\mathbf{1a}$. The O–H···O hydrogen bonding geometries, [O···O], [H···O] (Å), [O–H···O] (°), are (a) 2.6747(17), 1.80, 162; (b) 2.6462(18), 1.77, 163; (c) 2.7988(17), 2.02, 144; (d) 2.695(2), 1.81, 170; (e) 2.702(2), 1.86, 156. The geometries of the C–H···π contacts [H···π] (Å), [C–H···π] (°) are (f) 2.67, 142; (g) 2.58, 172.

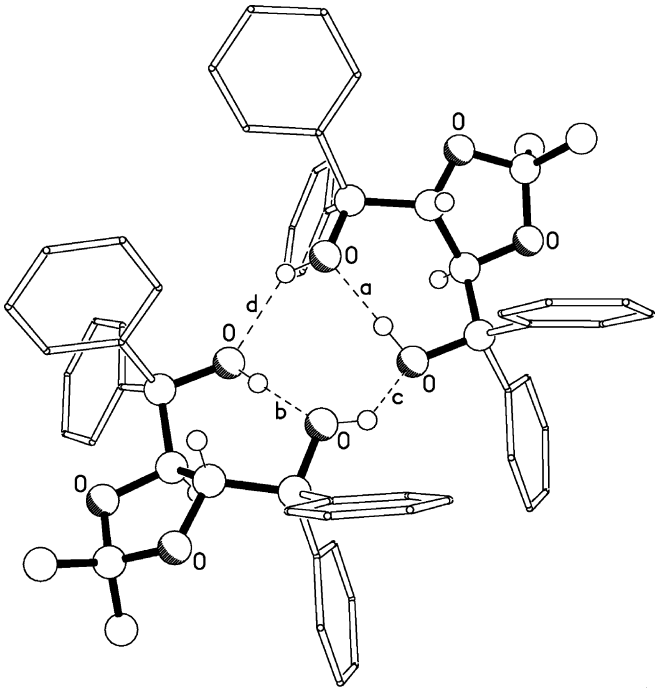

Figure 3. The molecular structure of SEWVUL01. The O–H···O hydrogen bonding geometries, [O···O], [H···O] (Å), [O–H···O] (°), are (a) 2.619, 1.73, 171; (b) 2.612, 1.72, 174; (c) 2.74, 2.04, 134; (d) 2.735, 2.05, 132 (O–H distances normalized to 0.90 Å).

hydrogen bonding cycle would not be directly affected by a change in the chirality at C(87) (all that would be required to change the chirality at this centre is swapping the locations of the hydride and methyl moieties). Thus, in order to explain the selective inclusion of guest **1a** within the host **2** matrix, the environment around and contacts formed by the hydride and the methyl must be considered. In fact both of these substituents form C–H···π hydrogen bonds to adjacent phenyl rings, one from each unique host **2** molecule (interactions f and g, respectively). The positions of the two host **2** molecules are such that if the hydride and methyl swapped places there would be a C–H···π contact from the new methyl group to an adjacent phenyl ring with an H···π separation of ca. 1.45 Å, clearly too short to be 'allowable'. Thus, the two host **2** molecules would have adopted a different mutual orientation to accommodate guest **1b**. We, therefore, suggest that the distortion in the host **2** framework necessary for the inclusion of guest **1b** would severely disrupt the energetically favourable O–H···O hydrogen bonding ring and thus disfavour the formation of an inclusion complex.

Table 1 shows equilibrium data for a range of resolutions. All resolutions exhibit selectivity towards (*S*)-enantiomer **1a**; virtually all of the (*R*)-enantiomer **1b** remains in the liquid phase uncomplexed. At a low concentration of the feed racemate (entries 1 and 2), the (*S*)-enantiomer concentration in the liquid remained constant at around 4 mM. However, as the feed racemate concentration was increased, the concentration of (*S*)-enantiomer in the liquid seemed to increase (entries 3–5). For a molar equivalent $\geqslant 1.0$, the resolutions exhibit the same values of ee (solid and liquid) and concentrations in the liquid (entries 6–9). At a molar equivalent of host = 0.5, more (*S*)-enantiomer was observed in the liquid phase presumably because the host added was insufficient to complex with the available (*S*)-enantiomer. The results of resolution for hexane and octane were comparable (entries 7 and 17) suggesting that there is no advantage in performing the resolution in a slightly more hydrophobic solvent. Practically, there is no significant improvement in ee by reducing the temperature (entries 14–16).

The decomplexation step is critical, and it is affected by the solvent mixture composition. Toluene was chosen as the decomplexation solvent since it is miscible with hexane and does not form hydrogen bonds with the host. We explored the possibility of running the resolution in toluene/hexane mixtures of varying compositions, to avoid having to revert to pure hexane at the end of each cycle (Step E in Fig. 1). Reverting to pure hexane would have required extensive diafiltration. Figure 4b shows that it is possible to run the resolution anywhere between 0 and 20 vol % toluene without sacrificing the enantiomeric excess (ee). At a high toluene composition there was insufficient host remaining as a solid (Fig. 4a) to form a complex, leading to a lower ee in the liquid. The complex completely dissociated into free enantiomers and host above 60 vol % toluene (Fig. 4c). Therefore, from the process point of view, it is not necessary to use either pure hexane for resolution (Step A), or pure toluene for decomplexation (Step D in Fig. 1).

Figure 5 provides a detailed description of a sequence of a set of resolution–filtration cycles. All operations were car-

Table 1. Effect of several parameters on the resolution of racemate **1** mediated by host **2**[a]

Entry	Initial substrate concentration (mM)	T (°C)	TADDOL (equiv)	Solvent	Concn of R in liquid (mM)	Concn of S in liquid (mM)	ee (%) of liquid (R)	ee (%) of solid (S)	Yield[b] of (S) in solid (%)
1	25	22	1.0	Hexane	14	4	54	93	1
2	50	22	1.0	Hexane	24	4	74	89	38
3	100	22	1.0	Hexane	51	7	75	85	74
4	200	22	1.0	Hexane	92	10	80	82	80
5	400	22	1.0	Hexane	191	21	80	80	80
6	50	22	0.5	Hexane	25	14	30	93	9
7	50	22	1.0	Hexane	24	4	74	89	38
8	50	22	1.5	Hexane	25	4	74	90	38
9	50	22	2.0	Hexane	25	4	73	86	41
10	50	22	1.0	Hexane	24	4	72	88	51
11	50	22	2.0	Hexane	25	4	74	88	32
12	100	22	1.0	Hexane	45	5	80	82	69
13	100	22	2.0	Hexane	45	4	82	82	58
14	50	5	1.0	Hexane	23	3	80	*83*	*90*
15	50	10	1.0	Hexane	23	3	81	*85*	*90*
16	50	22	1.0	Hexane	24	4	76	*87*	*87*
17	50	22	1.0	Octane	23	3	76	87	37
18	50	22	2.0	Octane	23	4	73	88	29

Note: For entries 14–16, solid ee and yield of S were calculated based on the initial moles fed and the moles in the liquid.
[a] The duration of resolution was 6 h.
[b] $\text{Yield} = \frac{S \text{ in solid}}{S \text{ fed}}$.

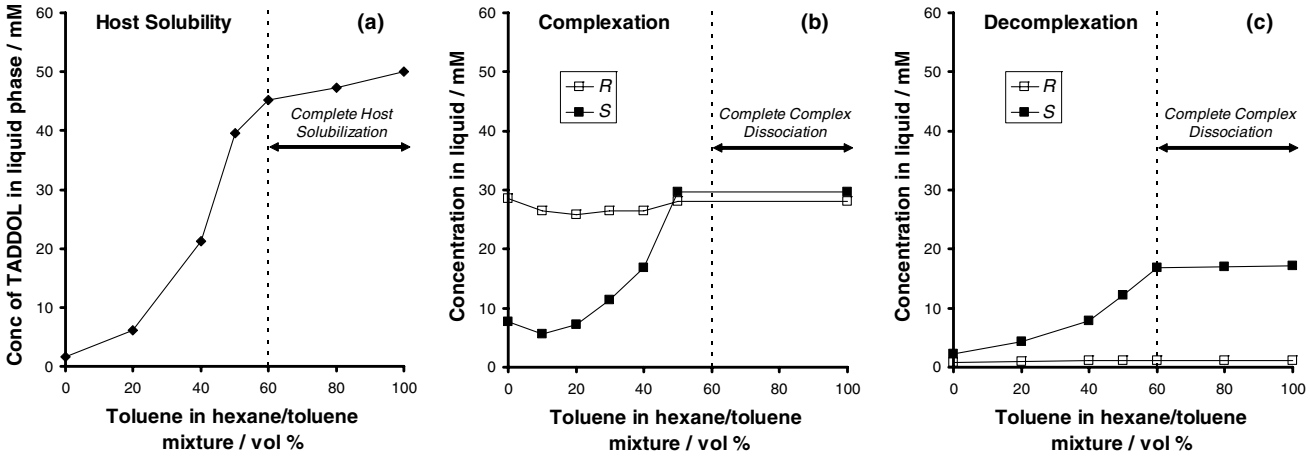

Figure 4. Solubilities as a function of solvent composition: (a) solubility of host **2**; (b) solubility of **1a** and **1b** with host **2** (complexation) and; (c) solubility of **1a** and **1b** when introduced as a solid complex with host **2**. Solid complex used in (c) was recovered from a resolution experiment employing **1** equivalent of host **2**.

ried out in a dead end nanofiltration cell. In the first cycle, racemate **1** (50 mM) was added to the cell containing host **2** (1 equiv) suspended in hexane and stirred. In the course of resolution, the (*S*)-enantiomer **1a** preferentially co-crystallized with the **2** and this led to an enrichment of (*R*)-enantiomer **1b** in the mother liquor (Step 1A). After 6 h of resolution, a pressure of 30 bar was applied and the liquid enriched with (*R*)-enantiomer permeated the membrane (Step $1B_1$). The solid complex was retained in the cell. In Steps $1B_2$ and $1B_3$, fresh hexane was added to the cell and two filtrations used to elute *R*-enantiomer. The combined permeate stream gave an enantiomeric excess of 46% (of *R*) and a yield[14] of 89% (of *R*). After virtually all of the dissolved (*R*)-enantiomer had been eluted out, toluene was added to take the mixture composition above 60 vol % toluene, above which the complex completely dissolves as (*S*)-enantiomer **1a** and host **2** (Step 1C). The cell was then pressurized and the (*S*)-enantiomer permeated the membrane, while the soluble host was retained (Step $1D_1$). Further decomplexation solvent (60% toluene) was then added to the cell for elution of the (*S*)-enantiomer (Step $1D_2$). The ee and yield of the combined permeate stream were 80% (of *S*) and 31% (of *S*), respectively. After the (*S*)-enantiomer had been eluted out, fresh hexane was added to the retentate to precipitate the host (Step 1E) and prepare it for the second cycle. To begin the second

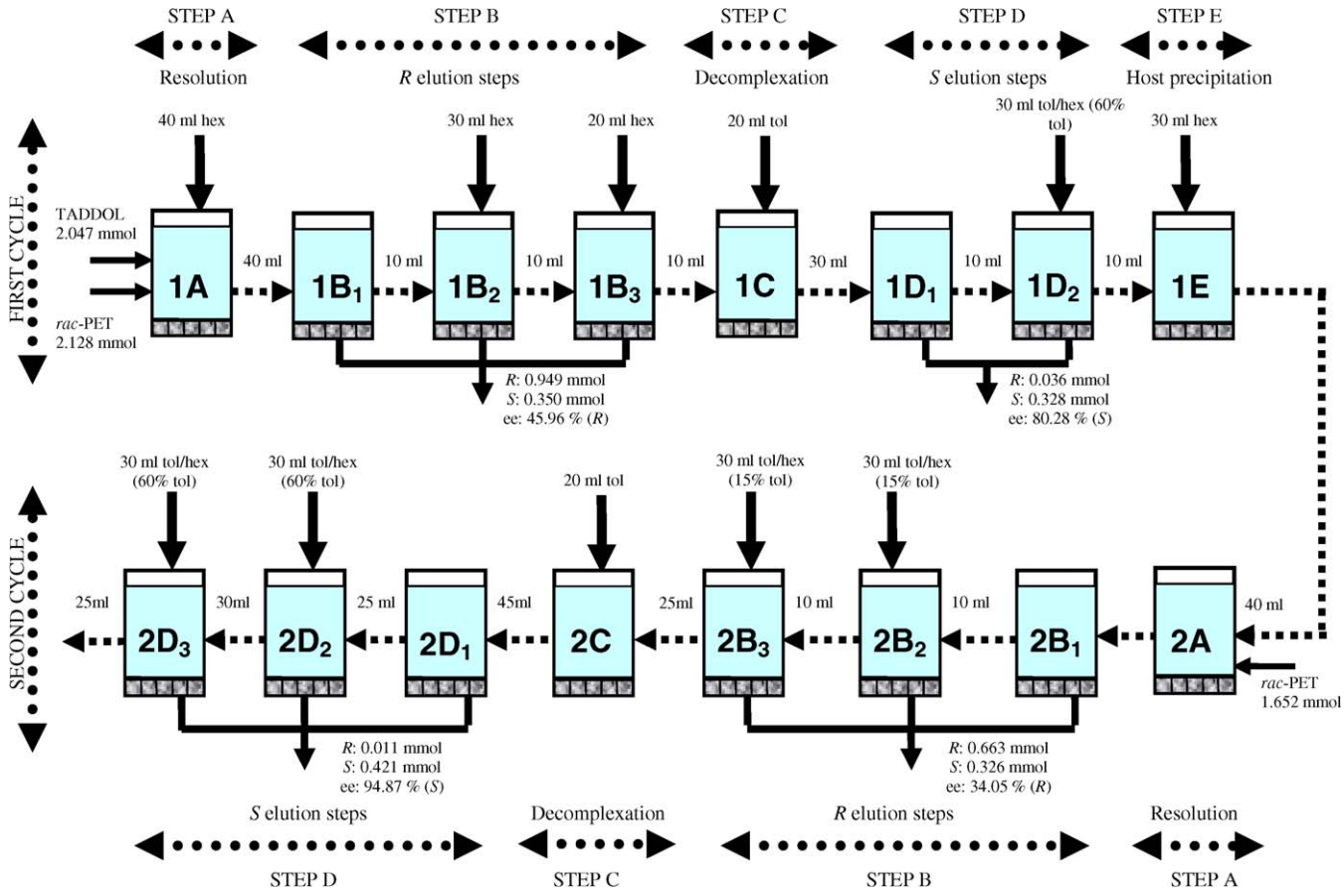

Figure 5. Process operations of enantioselective inclusion complexation–solvent decomplexation–OSN. Enantiomeric excess and moles of *R* and *S* in aggregated streams are shown.

cycle, fresh racemate was added to the host suspended in the cell to take the composition to 15 vol % toluene. Similar (*R*)- and (*S*)-elution steps were then executed. For the (*R*)-elution steps, the ee and the yield of the combined stream were 34% (of *R*) and 80% (of *R*), respectively. For the (*S*)-elution steps, the ee and the yield of the combined stream were 95% (of *S*) and 51% (of *S*), respectively. The elution profiles are shown in Figure 6. The enantioselectivity of the resolution was maintained at high ee (80% and 95% of *S*) in these two cycles, and, in principle, multiple cycles could be executed.

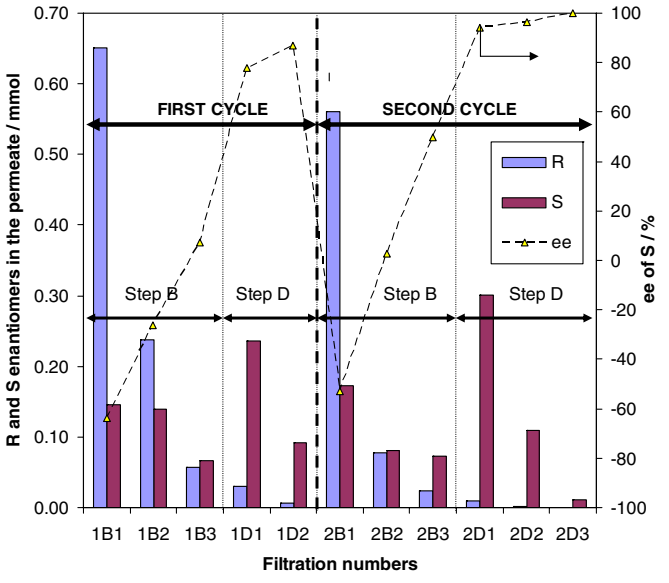

Figure 6. Elution profile of the resolution–filtration process and ee of the permeate stream in each filtration (indicated in Fig. 4) in two cycles. Step B is the elution of *R* and Step D is the elution of *S*. A positive ee indicates an (*S*)-rich permeate. A negative ee indicates an (*R*)-rich permeate.

3. Conclusions

A novel enantioseparation process using combined EIC–OSN has been demonstrated. We have shown for the first time that the use of solvent decomplexation and OSN allows enantiomer purification and the reuse/recycling of the chiral host. The strength of this process is the direct use of chiral host (without derivatization or immobilization), relatively high operating concentrations and ambient temperature processing. By selecting appropriate OSN membranes with a suitable MWCO it is possible to separate purified enantiomers and hosts. We regard the method presented here as having the potential as an alternative technique for preparative-scale chiral separations, which could extend the scope of EIC from the laboratory to the pilot and the industrial scale.

4. Experimental

4.1. General

Racemic **1** was obtained from Aldrich and host **2** was supplied by Fluka. HPLC grade solvents such as hexane and toluene were supplied by Fisher Scientific UK.

4.2. Analytical techniques

The enantiomers were analyzed by GC (Agilent, US) equipped with an HP-CHIRAL-20β (Agilent) column. Host concentration was measured by HPLC (Unicam, UK) with a Chiralcel OD-H (Daicel) column and using 90:10 (hexane/isopropanol) as the mobile phase.

4.3. Resolution–filtration procedure

A stainless steel SEPA ST (Osmonics, US) dead end nanofiltration cell with an effective membrane area of 13.9 cm^2 was employed as a resolution–filtration vessel. A membrane disk was clamped in place at the base of the cell. Membranes were preconditioned with approximately 400–500 ml of toluene in order to remove the lube oil preservative from the polymer and to compress the membrane at operating conditions. A typical procedure for resolution filtration was as follows. With a preconditioned membrane in place, 0.903 g of host **2** (2.047 mmol), hexane (40 ml) and *rac*-**1** (2.218 mol) were quickly added to the cell and the suspension formed was agitated. After 6 h, a pressure of 30 bar was applied (supplied by N_2 gas) and the permeate was collected for GC and HPLC analyses. After 75% of the initial liquid volume had permeated (about 30 ml), the cell was depressurized. Fresh solvent was added to the retentate (10 ml), and stirred for 30 min and then filtered again by pressurizing the cell (see Fig. 5). A similar procedure was used for the decomplexation step, but instead of adding hexane, toluene or toluene/hexane mixture was added. After elution of *R*, followed by decomplexation and elution of *S*, fresh racemate was added to the cell for the next cycle of resolution.

4.4. X-ray crystal structure analysis

Crystal data for inclusion complex $[\mathbf{2}]_2\cdot\mathbf{1a}$: $(C_{31}H_{30}O_4)_2\cdot C_8H_{10}O$, $M = 1055.26$, orthorhombic, $P2_12_12_1$ (no. 19), $a = 16.8753(5)$, $b = 16.8943(5)$, $c = 20.2579(6)$ Å, $V = 5775.5(3)$ Å^3, $Z = 4$, $\rho_{calcd} = 1.214$ g cm^{-3}, $\mu(Mo_{K\alpha}) = 0.079$ mm^{-1}, $T = 173$ K, colourless prismatic blocks, Oxford Diffraction Xcalibur 3 diffractometer; 19,946 independent measured reflections, F^2 refinement, $R_1 = 0.066$, $wR_2 = 0.156$, 19,271 independent observed absorption–corrected reflections [$|F_o| > 4\sigma(|F_o|)$, $2\theta_{max} = 65°$], 718 parameters. The absolute structure of inclusion complex $[\mathbf{2}]_2\cdot\mathbf{1a}$ could not be determined by either *R*-factor tests [$R_1^+ = 0.0659$, $R_1^- = 0.0659$] or by use of the Flack parameter [$x^+ = +0.4(6)$, $x^- = +0.6(6)$] and so was assigned using the known centre of the guest **1a** at C(87). CCDC 277087. The supplementary crystallographic data for this paper can be obtained free of charge via www.ccdc.cam.ac.uk/conts/retrieving.html (or from the Cambridge Crystallographic Data Centre, 12 Union Road, Cambridge CB21EZ, UK; fax: (+44) 1223-336-033; or deposit@ccdc.cam.ac.uk).

Acknowledgements

We thank Richard Sweeney (Department of Materials, Imperial College) for his technical help with the powder XRD analysis. N.F.G. acknowledges the financial support from the Ministry of Science, Technology and Innovation (MOSTI) of Malaysia.

References

1. (a) Kozma, D. *CRC Handbook of Optical Resolution via Diastereomeric Crystallisation*; CRC Press, 2002; (b) Collet, A. *Angew. Chem., Int. Ed.* **1998**, *37*, 3239–3241.
2. (a) Toda, F. *Pure Appl. Chem.* **2001**, *73*, 1137–1145; (b) Seebach, D.; Beck, A.; Heckel, A. *Angew. Chem., Int. Ed.* **2001**, *40*, 92–138; (c) Kaupp, G. *Angew. Chem., Int. Ed. Engl.* **1994**, *33*, 728–729; (d) Toda, F.; Tanaka, K. *J. Am. Chem. Soc.* **1983**, *105*, 5151–5152; (e) Weber, E.; Wimmer, C.; Llamas-Saiz, A. L.; Foces-Foces, C. *J. Chem. Soc., Chem. Commun.* **1992**, 733–735; (f) Tanaka, K.; Honke, S.; Urbanczyk-Lipkowska, Z.; Toda, F. *Eur. J. Org. Chem.* **2000**, 3171–3176; (g) Kassai, C.; Juvancz, Z.; Balint, J.; Fogassy, E.; Kozma, D. *Tetrahedron* **2000**, *56*, 8355–8359; (h) Grandeury, A.; Petit, S.; Gouhier, G.; Agasse, V.; Coquerel, G. *Tetrahedron: Asymmetry* **2003**, *14*, 2143–2152.
3. (a) Miyamoto, H.; Sakamoto, M.; Yoshioka, K.; Takaoka, R.; Toda, F. *Tetrahedron: Asymmetry* **2000**, *11*, 3045–3048; (b) Mori, K.; Toda, F. *Tetrahedron: Asymmetry* **1990**, *1*, 281–282; (c) Toda, F.; Takumi, H.; Tanaka, K. *Tetrahedron: Asymmetry* **1995**, *6*, 1059–1062.
4. (a) Legrand, S.; Luukinen, H.; Isaksson, R.; Kilpeläinen, I.; Lindström, M.; Nicholls, I.; Unelius, C. *Tetrahedron: Asymmetry* **2005**, *16*, 635–640; (b) Deng, J.; Chi, Y.; Fu, F.; Cui, X.; Yu, K.; Zhu, J.; Jiang, Y. *Tetrahedron: Asymmetry* **2000**, *11*, 1729–1732; (c) Bortolini, O.; Fantin, G.; Fogagnolo, M. *Chirality* **2005**, *17*, 121–130.
5. (a) Müller, S.; Afraz, M. C.; de Gelder, R.; Ariaans, G. J.; Kaptein, B.; Broxterman, Q. B.; Bruggink, A. *Eur. J. Org. Chem.* **2005**, 1082–1096; (b) Müller, S.; Ariaans, G. J.; Kaptein, B.; Broxterman, Q. B.; Bruggink, A. *Tetrahedron: Asymmetry* **2005**, *16*, 2535–2538.
6. (a) Toda, F. *Supramol. Sci.* **1996**, *3*, 139–148; (b) Toda, F.; Tanaka, K. *Tetrahedron Lett.* **1988**, *29*, 551–554.
7. Resolution using chiral host **2** and its derivatives: (a) Toda, F.; Tohi, Y. *J. Chem. Soc., Chem. Commun.* **1993**, 1238–1240; (b) Toda, F.; Tanaka, K.; Ootani, M.; Hayashi, A.; Miyahara, I.; Hirotsu, K. *J. Chem. Soc., Chem. Commun.* **1993**, 1413–1415; (c) von dem Bussche-Hunnefeld, C.; Beck, A.; Lengweiler, U.; Seebach, D. *Helv. Chim. Acta* **1992**, *75*, 438–441.
8. STARMEM™ 122 (W. R. Grace & Co., US) was kindly supplied by Membrane Extraction Technology (www.membrane-extraction-technology.com).
9. (a) Ghazali, N. F.; Patterson, D.; Livingston, A. *Chem. Commun.* **2004**, *8*, 962–963; (b) Luthra, S. S.; Yang, X.; dos Santos, L. M. F.; White, L. S.; Livingston, A. G. *Chem. Commun.* **2001**, *16*, 1468–1469; (c) Nair, D.; Scarpello, J. T.; White, L. S.; dos Santos, L. M. F.; Vankelecom, I. F. J.; Livingston, A. G. *Tetrahedron Lett.* **2001**, *42*, 8219–8222.
10. MWCO is obtained from the curve of the rejections (see Ref. 7) of a series of *n*-alkanes in toluene at 2 wt % versus their molecular weight, by defining the molecular weight corresponding to 90% rejection as the MWCO.

11. $$\text{Rejection } (\%) = 1 - \frac{\text{solute in permeate (mM)}}{\text{solute in retentate (mM)}} \times 100.$$

12. [SEWVUL01] Toda, F.; Tanaka, K.; Miyamoto, H.; Koshima, H.; Miyahara, I.; Hirotsu, K. *J. Chem. Soc., Perkin Trans. 2* **1997**, 1877–1886.

13. [LATCOY] Toda, F.; Tanaka, K.; Ootani, M.; Hayashi, A.; Miyahara, I.; Hirotsu, K. *J. Chem. Soc., Chem. Commun.* **1993**, 1413–1415.

14. $$\text{Yield } (\%) = \frac{\text{enantiomer in permeate (mol)}}{\text{enantiomer fed in the cycle (mol)}} \times 100.$$